

# Comparative Study of Convolution and Order Reduction Techniques for Blackbox Macromodeling Using Scattering Parameters

José E. Schutt-Ainé, *Fellow, IEEE*, Patrick Goh, Yidnekachew Mekonnen, *Member, IEEE*, Jilin Tan, *Senior Member, IEEE*, Feras Al-Hawari, Ping Liu, and Wenliang Dai

**Abstract**—In this paper, a fast convolution method using scattering parameters is presented for the macromodeling of blackbox multiport networks. The method is compared to model-order reduction passive macromodeling techniques in terms of robustness and computational efficiency. When scattering parameters are used as the transfer functions, convolution calculations can be accelerated to achieve superior performance and the resulting procedure leads to a robust, accurate, and efficient macromodel generation scheme. This paper examines the formulation of the convolution method. Model-order reduction techniques are reviewed and benchmark comparisons are performed.

**Index Terms**—Blackbox, causality, convolution, macromodel, passivity, scattering parameters, vector fitting.

## I. INTRODUCTION

WITH the advent of the computer age, circuit simulators have become invaluable tools in the design and development process of any electronic component. Circuit simulators provide developers with the ability to accurately predict the behavior of computer and communication networks before their actual implementation. Multiport networks characterized by sampled data or blackbox networks have become more frequent in the analysis or design of high-frequency or high-speed circuits. These systems offer significant challenges in the ability to accurately represent their behavior over a wide frequency range. In macromodel analysis, a complex network is described in terms of its terminal transfer functions in the frequency domain. This description consists of discrete data points obtained from a network analyzer or a full-wave field solver. A solution for the time-domain response can always be obtained by using convolution with the excitation provided at

its terminals, however, it has been believed that this approach is computationally inefficient and becomes prohibitive for large networks. To circumvent the time-consuming convolution calculations, model-order reduction (MOR) techniques that use curve fitting techniques have been employed to approximate blackbox data into a rational function in terms of poles and residues. These poles and residues are next used in a time-domain recursive convolution algorithm that is far more computationally efficient than a direct convolution approach. Several methods exist in the literature that describe the generation of these macromodels. These include methods based on rational approximation, Padé synthesis, and asymptotic waveform evaluation (AWE) [1]–[9]. More recently, these macromodel efforts have progressively converged to the vector fitting method [10] which is today the method of choice for approximating transfer functions of passive networks. Several enhancements of the vector fitting method have been proposed that aim at improving the accuracy, bandwidth, and computational complexity of the fitting process [11]–[15].

In many cases, the extraction of poles and residues of a multiport network can be tedious and cumbersome. For example, a typical serial link may require about 800 poles and residues to accurately approximate its transfer functions. Such a large order in the rational function approximation can nullify the use of recursive convolution. Furthermore, the poles and residues generated by the curve fitting process do not necessarily lead to a passive system. Consequently, passivity assessment and enforcement schemes must be imposed to the frequency domain representation before performing the time-domain simulation [16]–[20].

Commercial standard blackbox macromodels must be robust and the techniques for generating them must be efficient and reliable. In this paper, we propose a robust macromodeling scheme for the simulation of passive multiport networks. The method uses an accelerated convolution scheme that takes advantage of the fast decaying characteristics of scattering parameter representations. The paper is organized as follows. Section II presents a direct convolution formulation for multiport networks and a method for accelerating the convolution calculations. Section III discusses causality enforcement techniques. Section IV is an overview of MOR techniques and Section V shows benchmark comparisons between the two techniques.

Manuscript received July 1, 2010; revised June 15, 2011; accepted July 5, 2011. Date of publication September 19, 2011; date of current version October 12, 2011. Recommended for publication by Associate Editor M. Cases upon evaluation of reviewers' comments.

J. Schutt-Ainé and P. Goh are with the Electrical Engineering Department, University of Illinois at Urbana-Champaign, Urbana, IL 61801 USA (e-mail: jschutt@emlab.uiuc.edu; pgoh@illinois.edu).

Y. Mekonnen is with Intel Corporation, Chandler, AZ 85044 USA (e-mail: yidnekachew.s.mekonnen@intel.com).

J. Tan and F. Al-Hawari are with the Cadence Design Systems, Chelmsford, MA 01824 USA (e-mail: jtan@cadence.com; feras@cadence.com).

P. Liu and W. Dai are with the Cadence Design Systems, Shanghai 201203, China (e-mail: liuping@cadence.com; wldai@cadence.com).

Color versions of one or more of the figures in this paper are available online at <http://ieeexplore.ieee.org>.

Digital Object Identifier 10.1109/TCPMT.2011.2163308

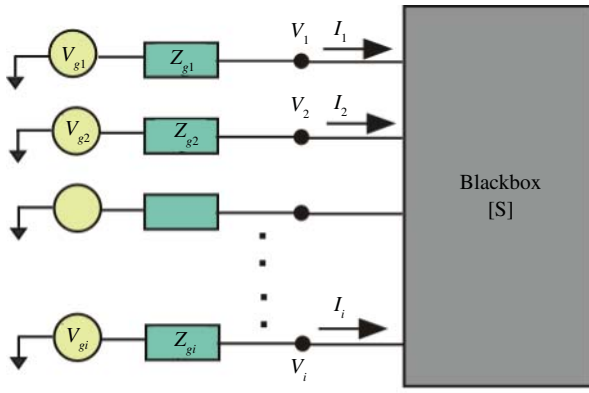


Fig. 1. Blackbox with termination and source.

## II. S-PARAMETER FORMULATION

In the frequency domain, the  $n$ -port linear blackbox S-parameter formulation reads (see Fig. 1)

$$\mathbf{B}(\omega) = \mathbf{S}(\omega)\mathbf{A}(\omega) \quad (1)$$

where  $\mathbf{A}(\omega)$  and  $\mathbf{B}(\omega)$  are vectors of length,  $n$  representing the incident and reflected voltage waves, respectively.  $\mathbf{S}(\omega)$  is an  $n \times n$  matrix containing the S-parameter transfer functions.

In the time domain, the scattering parameter formulation reads

$$\mathbf{b}(t) = \mathbf{s}(t) * \mathbf{a}(t) \quad (2)$$

where  $*$  indicates a convolution operation which is defined as

$$\mathbf{s}(t) * \mathbf{a}(t) = \int_{-\infty}^{\infty} \mathbf{s}(t - \tau) \mathbf{a}(\tau) d\tau. \quad (3)$$

When the time variable is discretized, the current time variable  $t$  is represented as  $t = M\Delta t$ , where  $\Delta t$  is the time step. Using the subscript  $d$  to denote discretized variables, the convolution becomes  $\mathbf{s}(t) * \mathbf{a}(t) = \mathbf{s}_d(M) * \mathbf{a}_d(M)$  or

$$\mathbf{s}_d(M) * \mathbf{a}_d(M) = \mathbf{s}_d(0) \mathbf{a}_d(M) \Delta t + \sum_{k=1}^M \mathbf{s}_d(k) \mathbf{a}_d(M - k) \Delta t \quad (4)$$

where  $\Delta t$  is the time step.  $M$  is the index associated with the current time. The time-domain scattering parameter formulation then reads

$$\mathbf{b}(t) = \mathbf{b}_d(M) = \mathbf{s}_{do} \mathbf{a}(t) + \mathbf{h}(t) = \mathbf{s}_{do} \mathbf{a}_d(M) + \mathbf{h}_d(M) \quad (5)$$

where  $\mathbf{s}_{do} = \mathbf{s}_d(0) \Delta t$ , and where  $\mathbf{h}(t)$  is a vector representing the history of the scattered voltage waves defined as

$$\mathbf{h}(t) = \mathbf{h}_d(M) = \sum_{k=1}^M \mathbf{s}_d(k) \mathbf{a}_d(M - k) \Delta t. \quad (6)$$

In addition, the incident and reflected waves can be related to the voltage and current measured at the terminals (Fig. 2)

$$\mathbf{a}(t) = \frac{1}{2} [\mathbf{v}(t) + \mathbf{Z}_o \mathbf{i}(t)] \quad (7)$$

and

$$\mathbf{b}(t) = \frac{1}{2} [\mathbf{v}(t) - \mathbf{Z}_o \mathbf{i}(t)] \quad (8)$$

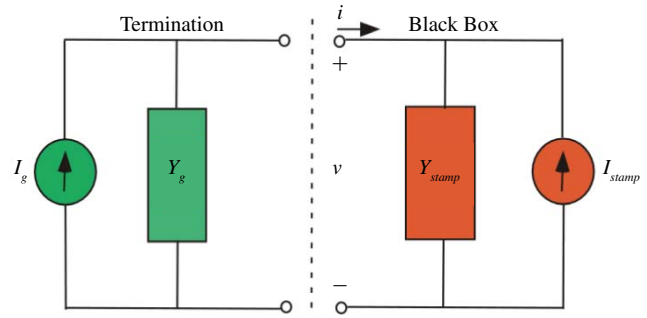


Fig. 2. Equivalent circuit at each time step.

where  $\mathbf{v}(t)$  and  $\mathbf{i}(t)$  are the terminal voltage and current vectors, respectively (dimension  $n$ ).  $\mathbf{Z}_o$  is the reference impedance matrix. Equations (7) and (8) can be combined with S-parameter equations to yield

$$\frac{1}{2} [\mathbf{v}(t) - \mathbf{Z}_o \mathbf{i}(t)] = \frac{1}{2} \mathbf{s}_{do} [\mathbf{v}(t) - \mathbf{Z}_o \mathbf{i}(t)] + \mathbf{h}(t). \quad (9)$$

After rearranging, we get

$$\mathbf{Z}_o \mathbf{i}(t) + \mathbf{s}_{do} \mathbf{Z}_o \mathbf{i}(t) + 2\mathbf{h}(t) = [\mathbf{1} - \mathbf{s}_{do}] \mathbf{v}(t) \quad (10)$$

or

$$[\mathbf{1} + \mathbf{s}_{do}] \mathbf{Z}_o \mathbf{i}(t) = [\mathbf{1} - \mathbf{s}_{do}] \mathbf{v}(t) - 2\mathbf{h}(t) \quad (11)$$

in which  $\mathbf{1}$  is the unit matrix of dimension  $n$ . From this, we get

$$\mathbf{i}(t) = \mathbf{Z}_o^{-1} [\mathbf{1} + \mathbf{s}_{do}]^{-1} [\mathbf{1} - \mathbf{s}_{do}] \mathbf{v}(t) - 2\mathbf{Z}_o^{-1} [\mathbf{1} + \mathbf{s}_{do}]^{-1} \mathbf{h}(t). \quad (12)$$

In most circuit simulators, the voltage-current relationship is expressed in the form of stamp parameters that represent subnetwork components. In this form (12) can be simplified to read

$$\mathbf{i}(t) = \mathbf{Y}_{stamp} \mathbf{v}(t) - \mathbf{i}_{stamp} \quad (13)$$

where

$$\mathbf{Y}_{stamp} = \mathbf{Z}_o^{-1} [\mathbf{1} + \mathbf{s}_{do}]^{-1} [\mathbf{1} - \mathbf{s}_{do}] \quad (14)$$

and

$$\mathbf{Y}_{stamp} = 2\mathbf{Z}_o^{-1} [\mathbf{1} + \mathbf{s}_{do}]^{-1} \mathbf{h}(t). \quad (15)$$

The solution for  $\mathbf{v}(t)$  is found using

$$(\mathbf{Y}_g + \mathbf{Y}_{stamp}) \mathbf{v}(t) = \mathbf{i}_g + \mathbf{i}_{stamp}. \quad (16)$$

$\mathbf{Y}_g$  and  $\mathbf{i}_g$  are the termination equivalent admittance matrix and source vectors, respectively, as shown in Fig. 2.

Most of the computational burden in the time-domain simulation rests on the calculation of  $\mathbf{h}(t)$  in (6), which involves expensive convolution operations. A typical approach, the inverse Fourier transform (IFFT) is used to generate the time-domain data. The computational complexity of convolution  $\mathbf{s} * \mathbf{a}$  is known to be  $O(n^2)$  where  $n$  is the number of points in discretized functions of  $\mathbf{s}$  and  $\mathbf{a}$ . Our approach to alleviate this problem takes advantage of the fact that scattering parameter impulse responses have relatively short durations and consist of pulses that decay very rapidly with time. A close observation of the time-domain scattering parameter data generated

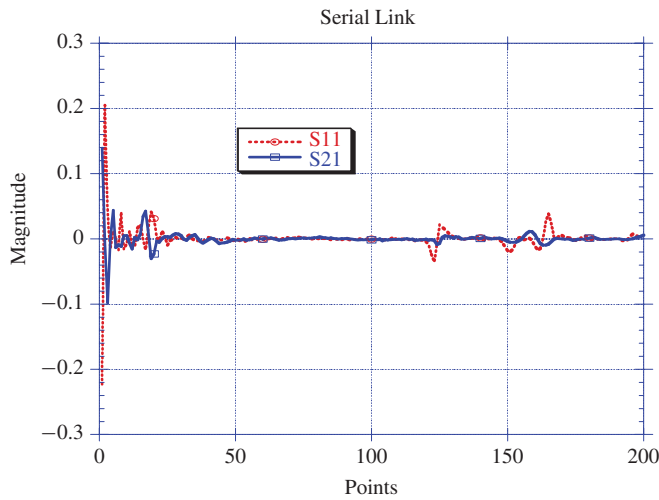


Fig. 3. Time-domain scattering parameter responses for a serial link showing the rapid decay of the function. Only the first 200 points from IFFT are shown.

by the IFFT shows that the vast majority of points have small magnitude and consequently, can be neglected.

More specifically, without loss of generality, (6) can be written in a scalar form as

$$h(t) = h_d(M) = \sum_{k=1}^M s_d(k) a_d(M-k) \Delta t \quad (17)$$

where  $s_d$ ,  $a_d$ , and  $h_d$  now refer to discretized scalar quantities associated with a scattering parameter, an incident wave, and the history of a reflected wave, respectively. Since most of the  $s_d(k)$  terms in the summation will be zeros, the calculation of  $h_d(M)$  can be accelerated dramatically. As a reformulation, we can assume that the discrete frequency-domain scattering parameter transfer functions can be described in the form

$$s_d(q) = \sum_{k=1}^L c_k e^{j2\pi qk} \quad (18)$$

in which the  $c_k$ 's and  $k$ 's are parameters to be determined.  $L$  is the order of the approximation that satisfies  $L \ll N$  where  $N$  is the total number of simulation points. With this representation, the associated time-domain function takes the form of a train of impulses whose weights are given by the  $c_k$ 's

$$s_d(u) = \sum_{k=1}^L c_k \delta(u-k). \quad (19)$$

The  $c_k$ 's are obtained by taking the inverse discrete Fourier transform or IFFT of the frequency-domain transfer function. If the transfer functions are scattering parameters, most of these  $c_k$ 's will be negligibly small and thus only a few ( $L$ ) will need to be retained for the representation described in (19). Convolution with an excitation function  $a_d(p)$  becomes

$$h_d(p) = \left[ \sum_{k=1}^L c_k \delta(p-k) \right] * a_d(p) = \sum_{k=1}^L c_k a_d(p-k). \quad (20)$$

For scattering parameters  $L$  is relatively small. For instance, the insertion loss scattering parameter of a backplane was

measured on a network analyzer up to 6 GHz. When the data are processed through a 1601-point IFFT, only 20 points of the resulting time-domain sequence are larger than 1% of the maximum (absolute) value. This can also easily be observed by looking at plots of the impulse response (Fig. 3). When the reference system is optimally chosen, the time-domain scattering parameters die out quickly, leading to very few points in the delta-function sequence. In general, the choice of  $L$  is directly predicated by the desired accuracy and is also a strong function of the frequency-domain data.

### III. CAUSALITY CONSIDERATIONS

Prior to performing the IFFT on the frequency-domain network parameters, we must insure that the data are suitable and satisfy conditions of passivity, causality, and realness. Most transfer functions used for blackbox multiport analysis are either obtained from network analyzer measurements or from full-wave electromagnetic solvers. Typically, the quantities obtained are scattering parameters which can be converted into other types of network parameters (Z or Y). Most network analyzers do not operate at very low frequencies and measured scattering parameters do not have DC data. Similarly, most full-wave field solvers suffer from serious inaccuracies at the lower frequencies and do not calculate DC transfer functions. DC extrapolation techniques must be used to generate data for the missing frequency points [21]. When data points are artificially added into actual data, one must insure that the physical properties of the system are not altered. For actual networks, the time-domain signals must exhibit certain properties that are associated with realizable systems. For instance, a signal in the time domain must be real, stable, and causal. Violation of these properties would lead to erroneous and non-physical solutions [22]–[24]. These properties lead to some important constraints to the time-domain signals and their associated frequency-domain responses.

Time-domain signals associated with physical networks must be causal [25]. This means that the response to an excitation starting at  $t = 0$  must be null for  $t < 0$

$$h(t) = 0, \quad t < 0 \quad (21)$$

where  $h(t)$  is the response of a system due to an excitation starting at  $t = 0$ .  $h(t)$  can be considered as the superposition of an even function and an odd function defined as

$$h_e(t) = \frac{1}{2} [h(t) + h(-t)] \quad \text{even function} \quad (22)$$

$$h_o(t) = \frac{1}{2} [h(t) - h(-t)] \quad \text{odd function.} \quad (23)$$

If  $h(t)$  is a causal function then

$$h_o(t) = \begin{cases} h_e(t), & t > 0 \\ -h_e(t), & t < 0 \end{cases} \quad (24)$$

or

$$h_o(t) = \text{sgn}(t) h_e(t). \quad (25)$$

Therefore,  $h(t)$  can be rewritten as

$$h(t) = h_e(t) + \text{sgn}(t) h_e(t). \quad (26)$$

In the frequency domain, this becomes

$$H(f) = H_e(f) - \frac{1}{j\pi f} * H_e(f). \quad (27)$$

It can be shown that the IFFT of the transfer function is given by

$$H(f) = H_e(f) - j\hat{H}_e(f) \quad (28)$$

where  $H(f)$  and  $H_e(f)$  are the transforms of  $h(t)$  and  $h_e(t)$ , respectively, and  $\hat{H}_e(f)$  is the Hilbert transform of  $H_e(f)$ . The Hilbert transform relationship is given by

$$\hat{x}(\xi) = x(\xi) * \frac{1}{\pi\xi} = \frac{1}{\pi} \int_{-\infty}^{+\infty} \frac{x(\tau)}{\xi - \tau} d\tau. \quad (29)$$

From this we see that in order for causality to exist, the imaginary part of the transform must be related to the real part through the Hilbert transform. When dealing with discrete data points, the discrete version of the Hilbert transform relationship is more appropriate. It is given by

$$\hat{f}_k = \begin{cases} \frac{2}{\pi} \sum_{n \text{ odd}} \frac{f_n}{k-n}, & k \text{ is even} \\ \frac{2}{\pi} \sum_{n \text{ even}} \frac{f_n}{k-n}, & k \text{ is odd.} \end{cases} \quad (30)$$

Relations (30) can be used to verify causality in the frequency-domain data. In actuality, causality is enforced by carrying the following steps. First, the real part of the frequency-domain data is inverted into the time domain via IFFT which yields the even part of the time-domain response. Next, the full time-domain response is generated from the even part using (26). This illustrates that the time-domain response can be generated entirely from the real part of the frequency-domain data [25].

#### IV. MOR APPROACH

Suppose we wish to evaluate the convolution operation

$$y(t) = v(t) * x(t) \quad (31)$$

where  $v(t)$  has the form of a decaying exponential function

$$v(t) = Ae^{-at}. \quad (32)$$

Using  $\Delta t$  as the time step, the convolution operation can be approximated as

$$y(t) = \int_0^t Ae^{-a\tau} x(t - \tau) d\tau; \frac{Ax(t - \Delta t)}{\alpha} + e^{-ah} y(t - \Delta t). \quad (33)$$

This is the recursive convolution algorithm which is substantially faster than the direct convolution operation [26], [27]. In order to exploit the advantages of the recursive convolution algorithm, one attempts to describe the transfer functions of the system under consideration to take a rational function form in the Laplace transform domain given by

$$H(s) = K + \sum_{i=1}^L \frac{\omega_{ci} a_i}{s + \omega_{ci}}. \quad (34)$$

In the time domain, this corresponds to an impulse response of the form

$$h(t) = K\delta(t) + \sum_{i=1}^L a_i \omega_{ci} e^{-\omega_{ci} t} \quad (35)$$

which can be used in a recursive convolution algorithm as expressed in (33). The  $a_i$ 's,  $\omega_{ci}$ 's, and  $K$  are residues, poles, and a constant, respectively.  $L$  is the order of the pole-residue approximation. If a blackbox transfer function can be processed to take the form shown in (34), the time-domain response can be calculated very efficiently using the recursive convolution algorithm of (33). The process of determining the poles and residues is central to MOR-based techniques.

Most macromodel construction methods are based on network partitioning, robust rational approximation, and recursive convolution in order to generate macromodels that can be used in time- and frequency-domain simulations. First, the network is partitioned into sub-networks. Next, accurate rational approximation methods are applied for complex systems to extract the poles and residues. Finally, the pole-residue level representations of lumped-model based and measured sub-networks are combined to form a global network. The pole-residue models are incorporated as sub-matrices into the system matrix of the global network using a recursive convolution formula. The entire system, including the nonlinear devices, is solved in the time domain. Thus, the size of the overall circuit to be simulated is reduced.

Several investigators have introduced algorithms and numerical techniques such as the AWE [1] for pole-residue identification. Work was later introduced to reduce the number of spurious poles generated by the reduction process. This includes the complex frequency hopping techniques [4], and the Krylov subspace methods [5], [6]. More recent work made use of orthogonal polynomials for more robust identification [28]. Although reliable models can be obtained from these techniques, in recent years preference has progressively converged to the vector fitting algorithm (VFIT) for system identification.

The VFIT has emerged as a method of choice in the generation of high-order rational functions over wide frequency ranges [10]. The method is an iterative technique based on pole relocation technique. It is shown that the iterative pole-relocation technique is the reformulation of the Sanathanan-Koerner iteration using partial fractions basis [14], [29].

The method has two main advantages, namely, numerical stability and convergence. It does not suffer from numerical problem when approximating high-order systems over a wide frequency range. It arrives at the optimal solution by solving two linear solutions with few iterations. Orthogonal vector fitting has been introduced in [14] to reduce the numerical sensitivity of the system equations to the choice of starting poles.

Once the poles and residues of a multiport network have been obtained, the time-domain impulse response can be directly obtained as shown in (31)–(35). Alternatively, a state-space representation can be used as described in [30]

$$\dot{\mathbf{x}}(t) = \mathbf{A}\mathbf{x}(t) + \mathbf{B}\mathbf{a}(t) \quad (36)$$

$$\mathbf{b}(t) = \mathbf{C}\mathbf{x}(t) + \mathbf{D}\mathbf{a}(t) \quad (37)$$

where  $A$  is an  $nL \times nL$  matrix containing the poles of the system,  $B$  is an  $nL \times n$  input mapping matrix,  $C$  is a matrix of dimension  $n \times nL$  containing the residues, and  $D$  is an  $n \times n$  matrix containing the direct coupling constants. These matrices are related to the scattering parameter matrix of the system via the relation

$$S(s) = C(sI - A)^{-1}B + D. \quad (38)$$

Although the system described by (34) can accurately describe the blackbox data at the sampled points, at frequency intervals not characterized by sample points, the analytical expression may be nonphysical. In particular, passivity violation may occur at these intervals. The passivity condition requires that a passive circuit does not create energy. Stable but nonpassive models may lead to unstable systems when connected to other passive systems leading to oscillation in the transient response. Passive macromodels, when terminated with any arbitrary passive load, always guarantee the stability of the overall network. Consequently, before treatment in the time domain, the pole-residue description given by (34) must be checked for passivity.

Most existing passivity enforcement techniques for curve-fitting methods are *a posteriori* methods based on first-order perturbation theory. In these methods, the transfer matrix is obtained from the curve-fitting methods accurately approximating the original frequency response over the entire frequency range. Then, the macromodel is checked for passivity violation frequency regions and perturbation method is applied to enforce passivity, assuming that only weak violations of passivity occur in the constructed macromodel.

Since poles are characteristic frequencies of the system, common poles can be used to represent the multiport passive system when approximating by rational function matrix  $H(s)$ . Different approaches are available to enforce passivity. Some of these approaches are frequency range dependent. In [20], an eigenvalue approach has been discussed, which enforces passivity of the macromodel by directly compensating the poles and residues of the rational function using linearization and constrained minimization through quadratic programming. However, this method that is based on searching the frequency band of violation, is computationally expensive and uses discrete, band-limited frequency samples for enforcing passivity of the macromodel. Hence, the generated macromodel can still violate passivity over a continuous frequency and outside the band-limited frequency response since the macromodel is tested at discrete frequency samples.

Recently, the rational function matrix  $H(s)$  has been used to represent the passive macromodel for multiport circuits, and a compensation method has been proposed [31]. The compensation method can detect the frequency band violating passivity using the associated Hamiltonian matrix. From the state-space representation and using  $A$ ,  $B$ ,  $C$ , and  $D$ , the Hamiltonian matrix  $M$  of an  $n$ -port system can be constructed as

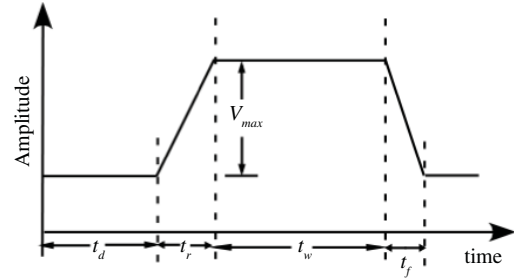
$$M = \begin{bmatrix} A - BR^{-1}D^T C & -BR^{-1}B^T \\ C^T S^{-1}C & -A^T + C^T DR^{-1}B^T \end{bmatrix} \quad (39)$$

where

$$R = (D^T D - I) \text{ and } S = (DD^T - I). \quad (40)$$

TABLE I  
DATA FILE DESCRIPTION

Name	Ports	Description
Blackbox-1	2	2-port I/O network – 1 MHz – 5 GHz
Blackbox-2	2	Microstrip line: 50 MHz – 7 GHz
Blackbox-3	2	Microstrip Coupler: 50 MHz – 5 GHz
Blackbox-4	2	Microstrip on FR4 2 GHz – 50 GHz
Blackbox-5	2	Lossy microstrip line: 0 – 20 GHz
Blackbox-6	2	18-inch meander 300 KHz – 6 GHz
Blackbox-7	4	4-port data A:50 MHz – 20.05 GHz
Blackbox-8	4	4-port data B 0 – 50 GHz
Blackbox-9	4	4-port data C:50 MHz – 20.05 GHz



Input pulse:

- time delay:  $t_d = 10$  ns
- rise time:  $t_r = 1$  ns
- fall time:  $t_f = 1$  ns
- pulse width:  $t_w = 8$  ns
- pulse amplitude:  $V_{max} = 1$  V

Fig. 4. Input pulse parameters.

The system is passive if  $M$  has no purely imaginary eigenvalues. Passivity violation analysis is performed by determining the frequency ranges in which the system is not passive. If imaginary eigenvalues are found, they define the crossover frequencies at which the system switches from passive to nonpassive (or vice versa). The crossover points give the frequency bands where passivity is violated.

The Hamiltonian matrix  $M$  has dimension  $2nL \times 2nL$ . For a 4-port circuit with VFIT order of 80,  $M$  will be of dimension  $2 \times 4 \times 80 = 640$ . Techniques have been proposed that use symmetry and reciprocity of networks to speed up these calculations [32]. Passivity enforcement can be performed by perturbing either the poles or the residues of the system. In [30], the residues are perturbed by adding increment  $\Delta C$  to the residue matrix  $C$ . Next, a relationship between  $\Delta C$  and the change in the eigenvalues of the dissipation matrix  $\Delta \lambda$  is established so as to solve an inverse perturbation problem. This is accomplished by minimizing the quantity

$$\|\Delta S\|^2 = \text{vec}(\Delta C)^T \text{vec}(\Delta C) \quad (41)$$

subject to the constraint

$$\Delta \lambda = G \text{vec}(\Delta C) \quad (42)$$

where  $\text{vec}(X)$  denotes the vectorization of the matrix  $X$  formed by stacking the columns of  $X$  into a single column.  $\|\Delta S\|^2$  is the norm associated with the resulting changes in the scattering

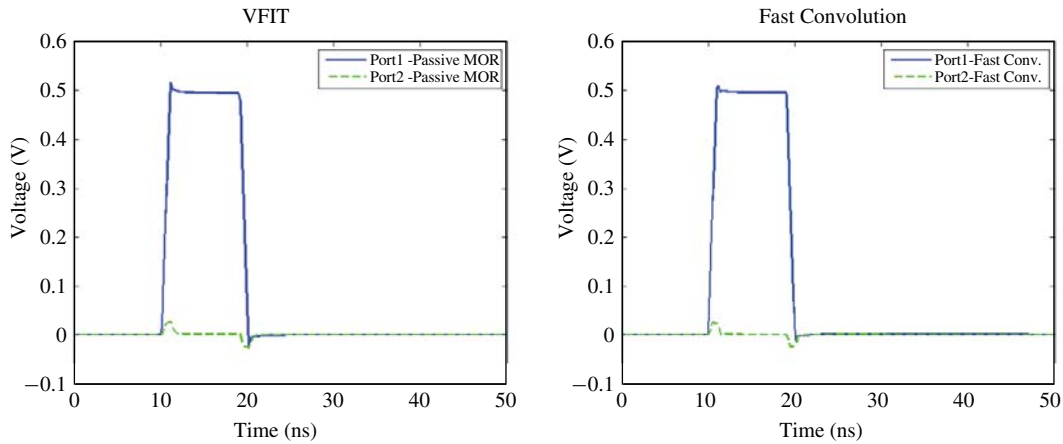
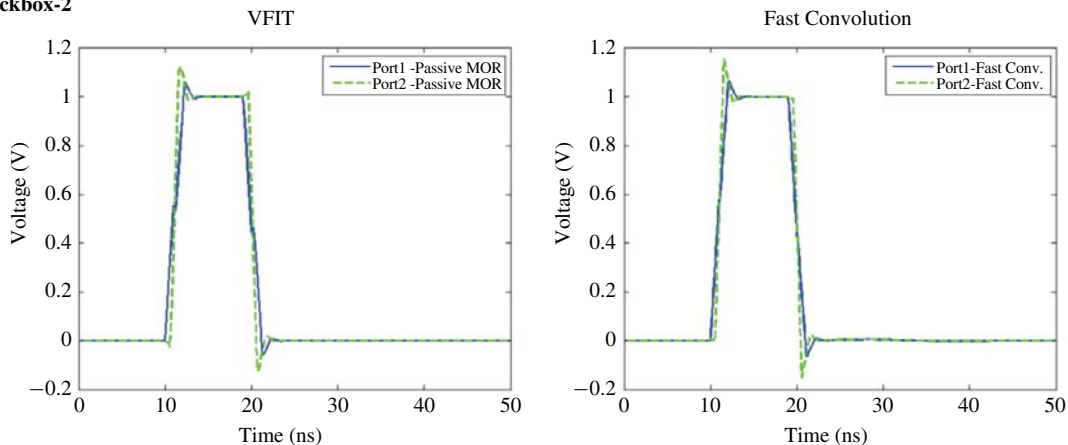
**Blackbox-1****Blackbox-2**

Fig. 5. Simulation comparisons for VFIT and fast convolution.

parameter matrix.  $\mathbf{G}$  is a  $U \times n^2L$  rectangular matrix ( $U =$  number of maximum violation points) that is constructed from the dissipation matrices of the perturbed and unperturbed systems. Details for the construction of  $\mathbf{G}$  can be found in [30] and are not repeated here. Equations (41) and (42) can be combined in a quadratic program to solve for  $\text{vec}(\Delta\mathbf{C})$ . The resulting matrix  $\mathbf{C}' = \mathbf{C} + \Delta\mathbf{C}$  can be used to construct the macromodel for the passive system.

#### V. TIME-DOMAIN SIMULATION - BENCHMARKS

In order to compare the accuracy, robustness, and computational efficiency of the convolution and MOR-based techniques, several time-domain transient simulations were performed for various two-port and four-port networks. Two computer programs were generated. The first program used the MOR-VFIT approach described in Section IV. The speed of the pole identification process was further enhanced using the method described in [15]. Passivity assessment was performed using the Hamiltonian approach described in [31]. Passivity enforcement was done using the method described in [30].

For the convolution program, the method described in (1)–(20) was combined with the DC extrapolation and causality enforcement procedures described in (21)–(30). A causal IFFT routine was used before using the fast convolution technique described in Section III.

The excitation used was a pulse with characteristics shown in Fig. 4. The simulation time was 50 ns. In all cases, the excitation was provided in port 1, using a generator with a 50-ohm internal impedance. All the other ports were left open. Since the fast convolution method is based on IFFT, caution must be taken in properly choosing *a priori* the parameters of the excitation signal. A relationship must exist between the bandwidth of the blackbox data and the signal of interest. In particular, the signal should not contain frequency components above the highest frequency of data available.

Table I shows a description of various data files used for the benchmark procedure. The files were obtained from network analyzer measurements or from full-wave electromagnetic field solvers.

Fig. 5 shows comparisons of plots of waveforms using both methods for a 1ns-rise time pulse for Blackbox 1 and Blackbox 2. Table II shows the benchmarks for the simulation. The platform used for the simulations was Visual C running on an AMD 2.3 GHz Dual Core processor with 1 GB of RAM. In the MOR case, the simulation time for vector fitting, passivity enforcement and recursive convolutions are shown separately. In some cases, fitting with different orders for VFIT are shown to illustrate the effects on speed.

For MOR-based method, the order of the approximation  $L$  in the partial fraction expansion is critical in determining

TABLE II  
BENCHMARK FOR MOR AND FAST CONVOLUTION TECHNIQUES

Data file	No. of points	MOR with Vector Fitting					Fast Convolution
		Order	Time (s)				Time (s)
			VFIT <sup>‡</sup>	Passivity Enforcement	Recursive Convolution <sup>#</sup>	TOTAL	
Blackbox 1	501	10*	0.14	0.01 <sup>NV</sup>	0.02	0.17	<b>0.078</b>
Blackbox 2	802	20*	0.41	5.47	0.03	5.91	<b>0.110</b>
Blackbox 3	802	40*	1.08	0.08 <sup>NV</sup>	0.06	1.22	<b>0.125</b>
Blackbox 4	802	60*	2.25	1.89	0.09	4.23	<b>0.125</b>
		100	3.17	5.34	0.16	8.67	
Blackbox 5	2002	50*	4.97	0.09 <sup>NV</sup>	0.28	5.34	<b>0.328</b>
Blackbox 6	802	100*	3.17	0.56 <sup>NV</sup>	0.16	3.89	<b>0.109</b>
Blackbox 7	1601	100*	24.59	28.33	1.31	53.23	<b>0.438</b>
		120	31.16	27.64	1.58	60.38	
Blackbox 8	5096	220	250.08	25.77 <sup>NV</sup>	10.05	285.90	<b>2.687</b>
Blackbox 9	1601	200*	58.47	91.63	2.59	152.69	<b>0.469</b>
		250	80.64	122.83	3.22	206.69	
		300	106.53	61.58 <sup>NV</sup>	3.86	171.97	

\* Lowest order for a visually good fit, rounded up to the nearest 10.

<sup>‡</sup> 2 iterations of VFIT done.

<sup>NV</sup> No violation. No passivity enforcement necessary. Time needed was to check passivity.

<sup>#</sup> Time for one simulation up to  $Num\_time = 2 * Num\_freq$ . Time step was chosen such that the total simulation time is 50 ns.

the speed and accuracy of the simulation results. The computational advantage gained through the use of recursive convolution may be lost if the order is high. In addition, it was observed that for the most part passivity enforcement contributed to the computational time and represented an important fraction of the total time. This is due to the process of iteratively determining the eigenvalues of the Hamiltonian and in perturbing the residue matrix for enforcement.

The results summarized in Table II as well as numerous additional simulations permit us to conclude that an MOR-based technique for blackbox macromodeling does not offer a significant advantage over convolution-based methods. In fact, if scattering parameters are used, fast convolution can be used to accelerate the simulation. All simulations indicated that reliable and comparable accuracy can be obtained by both convolution and MOR techniques. In both cases, the order is essential in determining the computational speed.

In the case of the VFIT MOR approach, the run times are split to show the values for the curve fitting, passivity enforcement, and recursive convolution separately. It is first observed that if the approximation order is high, the recursive convolution method can lose its advantage over the plain convolution approach. To fully harness the advantages of recursive convolution, it is imperative that the approximation order be kept low. A high order will not only reduce the efficiency of the recursive convolution scheme but also exacerbate the computational burden associated with the passivity assessment and enforcement procedures.

## VI. CONCLUSION

This paper performed a comparative analysis of blackbox macromodeling techniques. MOR techniques based on the vector-fitting method were reviewed as well as passivity

enforcement/assessment techniques. This paper also presented a fast convolution technique based on the scattering parameter representation of the blackbox. Frequency-domain preprocessing of blackbox data and simple  $\delta$ -function representation of the time-domain scattering parameter impulse responses resulted in a robust, accurate, and efficient macromodeling procedure. Time-domain scattering parameters are impulse responses that die out very rapidly because the traveling power waves are for the most part absorbed into the reference system. By utilizing this property, the time-domain convolution burden can be significantly reduced without significant alteration of the initial blackbox data. Since the method simply involves an IFFT and delta-function convolutions, its implementation is relatively easy. Benchmark results showed significant advantage of this fast convolution method over MOR. This paper also demonstrates that although recursive convolution is a very fast algorithm, the advantage in using it can be lost if the order from the reduction process is high. Moreover, pole/residue identification, passivity assessment/enforcement add to the computational burden and can lead to significant slowdown of the simulation. Finally, inaccuracies may occur in both MOR and convolution techniques as a result of passivity and causality enforcements. These inaccuracies are strongly dependent on the quality of the original blackbox data.

## REFERENCES

- [1] L. T. Pillage and R. A. Rohrer, "Asymptotic waveform evaluation for timing analysis," *IEEE Trans. Comput.-Aid. Des.*, vol. 9, no. 4, pp. 352–366, Apr. 1990.
- [2] J. Bracken, V. Raghavan, and R. Rohrer, "Interconnect simulation with asymptotic waveform evaluation (AWE)," *IEEE Trans. Circuits Syst.*, vol. 39, no. 11, pp. 869–878, Nov. 1992.
- [3] T. Tang and M. Nakhla, "Analysis of lossy multiconductor transmission lines using the asymptotic waveform evaluation technique," *IEEE Trans. Microw. Theory Tech.*, vol. 39, no. 12, pp. 2107–2116, Dec. 1991.

- [4] E. Chiprout and M. S. Nakhla, "Analysis of interconnect networks using complex frequency hopping (CFH)," *IEEE Trans. Comput.-Aid. Des.*, vol. 14, no. 2, pp. 186–200, Feb. 1995.
- [5] P. Feldmann and R. W. Freund, "Efficient linear circuit analysis by Pade approximation via the Lanczos process," *IEEE Trans. Comput.-Aid. Des. Integr. Circuits Syst.*, vol. 14, no. 5, pp. 639–649, May 1995.
- [6] M. Celik and A. C. Cangellaris, "Simulation of dispersive multiconductor transmission lines by Pade approximation via the Lanczos process," *IEEE Trans. Microw. Theory Tech.*, vol. 44, no. 12, pp. 2525–2535, Dec. 1996.
- [7] W. T. Beyene and J. E. Schutt-Ainé, "Accurate frequency-domain modeling and efficient circuit simulation of high-speed packaging interconnects," *IEEE Trans. Microw. Theory Tech.*, vol. 45, no. 10, pp. 1941–1947, Oct. 1997.
- [8] A. Odabasioglu, M. Celik, and L. Pillegi, "PRIMA: Passive reduced-order interconnect macromodeling algorithm," in *Proc. Int. Conf. Comput.-Aid. Des.*, Nov. 1997, pp. 58–65.
- [9] Q. Yu, J. Wang, and E. Kuh, "Passive multipoint moment matching model order reduction algorithm on multipoint distributed interconnect networks," *IEEE Trans. Circuits Syst. I: Fundam. Theory Appl.*, vol. 46, no. 1, pp. 140–160, Jan. 1999.
- [10] B. Gustavsen and A. Semlyen, "Rational approximation of frequency domain responses by vector fitting," *IEEE Trans. Power Del.*, vol. 14, no. 3, pp. 1052–1061, Jul. 1999.
- [11] B. Gustavsen, "Improving the pole relocating properties of vector fitting," *IEEE Trans. Power Del.*, vol. 21, no. 3, pp. 1587–1592, Jul. 2006.
- [12] Y. S. Mekonnen and J. E. Schutt-Ainé, "Broadband macromodeling of sampled frequency data using  $z$ -domain vector-fitting method," in *Proc. 11th IEEE Workshop Signal Propagat. Interconn.*, Genova, Italy, May 2007, pp. 45–48.
- [13] Y. S. Mekonnen and J. E. Schutt-Ainé, "Fast macromodeling technique of sampled time/frequency data using  $z$ -domain vector-fitting method," in *Proc. IEEE 16th Topical Meet. Electr. Perform. Electron. Packag.*, Atlanta, GA, Oct. 2007, pp. 47–50.
- [14] D. Deschrijver, B. Haegeman, and T. Dhaene, "Orthonormal vector fitting: A robust macromodeling tool for rational approximation of frequency domain responses," *IEEE Trans. Adv. Packag.*, vol. 30, no. 2, pp. 216–225, May 2007.
- [15] D. Deschrijver, M. Mrozowski, T. Dhaene, and D. De Zutter, "Macromodeling of multipoint systems using a fast implementation of the vector fitting method," *Microw. Wireless Compon. Lett.*, vol. 18, no. 6, pp. 383–385, Jun. 2008.
- [16] D. Saraswat, R. Achar, and M. Nakhla, "Global passivity enforcement algorithm for macromodels of interconnect subnetworks characterized by tabulated data," *IEEE Trans. Very Large Scale Integr. Syst.*, vol. 13, no. 7, pp. 819–832, Jul. 2005.
- [17] A. Lamecki and M. Mrozowski, "Equivalent SPICE circuits with guaranteed passivity from nonpassive models," *IEEE Trans. Microw. Theory Tech.*, vol. 55, no. 3, pp. 526–532, Mar. 2007.
- [18] B. Gustavsen and A. Semlyen, "Enforcing passivity for admittance matrices approximated by rational functions," *IEEE Trans. Power Syst.*, vol. 16, no. 1, pp. 97–104, Feb. 2001.
- [19] P. Triverio, S. Grivet-Talocia, M. S. Nakhla, F. G. Canavero, and R. Achar, "Stability, causality, and passivity in electrical interconnect models," *IEEE Trans. Adv. Packag.*, vol. 30, no. 4, pp. 795–808, Nov. 2007.
- [20] S.-H. Min and M. Swaminathan, "Efficient construction of two-port passive macromodels for resonant networks," in *Proc. IEEE 10th Electr. Perform. Electron. Packag.*, Cambridge, MA, Oct. 2001, pp. 229–232.
- [21] J. Schutt-Ainé, J. Tan, and C. Kumar, "Use of Smith chart to compensate for missing data on network performance at lower frequency," U.S. Patent 06 140, Oct. 2007.
- [22] R. Mandrekar and M. Swaminathan, "Causality enforcement in transient simulation of passive networks through delay extraction," in *Proc. 9th IEEE Workshop Signal Propagat. Interconn.*, May 2005, pp. 25–28.
- [23] F. M. Tesche, "On the use of the Hilbert transform for processing measured CW data," *IEEE Trans. Electromagn. Compat.*, vol. 34, no. 3, pp. 259–266, Aug. 1992.
- [24] S. Narayana, T. K. Sarkar, R. Adve, M. Wicks, and V. Vannicola, "A comparison of two techniques for the interpolation/extrapolation of frequency domain responses," *Digital Signal Process. J.*, vol. 6, pp. 51–67, Feb. 1996.
- [25] A. V. Oppenheim and R. W. Schaffer, *Discrete-Time Signal Processing*. Upper Saddle River, NJ: Prentice-Hall, 1999.
- [26] A. Semlyen and A. Dabuleanu, "Fast and accurate switching transient calculations on transmission lines with ground return using recursive convolutions," *IEEE Trans. Power Appar. Syst.*, vol. 94, no. 2, pp. 561–571, Mar. 1975.
- [27] D. Saraswat, R. Achar, and M. Nakhla, "Restoration of passivity in  $S$ -parameter data of microwave measurements," in *Proc. IEEE Int. Microw. Symp.*, Long Beach, CA, Jun. 2005, pp. 1–4.
- [28] R. Gao, Y. S. Mekonnen, W. Beyene, and J. E. Schutt-Ainé, "Black-box modeling of passive systems by rational function approximation," *IEEE Trans. Adv. Packag.*, vol. 28, no. 2, pp. 209–215, May 2005.
- [29] C. K. Sanathanan and J. Koerner, "Transfer function synthesis as a ratio of two complex polynomials," *IEEE Trans. Autom. Control*, vol. 8, no. 1, pp. 56–58, Jan. 1963.
- [30] D. Saraswat, R. Achar, and M. Nakhla, "A fast algorithm and practical considerations for passive macromodeling of measured/simulated data," *IEEE Trans. Adv. Packag.*, vol. 27, no. 1, pp. 57–70, Feb. 2004.
- [31] S. Grivet-Talocia, "Passivity enforcement via perturbation of Hamiltonian matrices," *IEEE Trans. Circuits Syst. I*, vol. 51, no. 9, pp. 1755–1769, Sep. 2004.
- [32] B. Gustavsen and A. Semlyen, "Fast passivity assessment for  $S$ -parameter rational models via a half-size test matrix," *IEEE Trans. Microw. Theory Tech.*, vol. 56, no. 12, pp. 2701–2708, Dec. 2008.



**José E. Schutt-Ainé** (S'86–M'86–SM'98–F'07) received the B.S. degree in electrical engineering from the Massachusetts Institute of Technology, Cambridge, in 1981, and the M.S. and Ph.D. degrees from the University of Illinois at Urbana-Champaign (UIUC), Urbana, in 1984 and 1988, respectively.

He joined Hewlett-Packard Technology Center, Santa Rosa, CA, as an Application Engineer involved with microwave transistors and high-frequency circuits. In 1983, he joined UIUC, and then joined the Electrical and Computer Engineering Department as a member of the Electromagnetics and Coordinated Science Laboratories, where he currently specializes in the study of signal integrity for high-speed digital and high-frequency application. He has been a consultant for several corporations. His current research interests span the spectrum from microwave measurements to the generation of computer-aided design tools for electronic systems.

Dr. Schutt-Ainé was the recipient of several research awards including the National Science Foundation (NSF) MRI Award in 1991, the National Aeronautics and Space Administration (NASA) Faculty Award for Research in 1992, the NSF MCAA Award in 1996, and the UIUC–National Center for Superconducting Applications (NSCA) Faculty Fellow Award in 2000. He is currently serving as Editor-in-Chief of the IEEE TRANSACTIONS ON COMPONENTS, PACKAGING, AND MANUFACTURING TECHNOLOGY.



**Patrick Goh** received the B.S. and M.S. degrees in electrical engineering from the University of Illinois at Urbana-Champaign (UIUC), Urbana, in 2007 and 2009, respectively, where he is currently pursuing the Ph.D. degree.

He has been with the Department of Electrical and Computer Engineering, UIUC, since August 2007, as a Teaching Assistant. His current research interests include circuit simulation for high-speed interconnects, modeling, and computer-aided design tools.

Mr. Goh is a reviewer of the IEEE TRANSACTIONS ON ADVANCED PACKAGING and the IEEE TRANSACTIONS ON COMPONENTS, PACKAGING, AND MANUFACTURING TECHNOLOGY.



**Yidnekachew S. Mekonnen** (S'02–M'08) was born in Addis Ababa, Ethiopia. He received the B.S. degree in electrical and computer engineering from Addis Ababa University, Addis Ababa, in 2000, and the M.S. and Ph.D. degrees in electrical and computer engineering from the University of Illinois at Urbana-Champaign, Urbana, in 2004 and 2007, respectively.

He was with Cadence Design Systems, Chelmsford, MA, as a Summer Intern, and IBM T. J. Watson Research Center, Yorktown Heights, NY, in 2005 and 2006, respectively. In 2008, he joined Intel Corporation, Chandler, AZ, as an Electrical Packaging Engineer. His current research interests include silicon-package co-design and technology development, signal and power integrity, high-frequency circuit simulation and high-speed input/output circuits, and channel designs.



**Jilin Tan** (SM–07) received the M.S. degree in theoretical physics from Beijing Normal University, Beijing, China, in 1986, and the Ph.D. degree in electrical engineering from the University of Wisconsin, Milwaukee, in 1994, followed by a one-year post-doctoral study in Arizona State University, Tempe.

He joined Compact Software, Inc. (later Compact Division of Ansoft Corporation), Elmwood Park, NJ, as a Research and Development Engineer, in 1996.

After one year with Intel Corporation, Hillsboro, OR, as a Senior Signal Integrity Engineer, he joined Cadence Design Systems, Inc., Chelmsford, MA, as a Senior Member of Consulting Staff, in 2000, and became an Architect in 2005. His current research interests include signal integrity analysis, advanced electromagnetic modeling and simulation of interconnects in high-speed digital printed circuit board and packaging.

Dr. Tan is an Associate Editor of the IEEE TRANSACTIONS ON ADVANCED PACKAGING. He has been coordinating the Cadence-University of Illinois at Urbana-Champaign Joint Program since 2006.



**Feras Al-Hawari** received the B.S. degree in electrical engineering from the Jordan University of Science and Technology, Irbid, Jordan, in 1993, the M.S. degree in computer engineering from the Florida Institute of Technology, Melbourne, in 1995, and the Ph.D. degree in electrical engineering from Northeastern University, Boston, MA, in 2007.

He is currently a Senior Member of Consulting Staff as well as a Technical Lead for the circuit simulation and signal integrity (SI) analysis technologies in the Allegro Printed Circuit Board SI Research and Development Group, Cadence Design Systems, Chelmsford, MA. Recently, he developed efficient and accurate methods to model and simulate S-parameters blackboxes, multi-conductor transmission lines, and input output buffer information specification input/output (I/O) devices. In 1995, he joined Cadence Design Systems. He also architected the bus analysis flow that is used to design and verify source synchronous memory interfaces such as double data rate type three. He also filed six patents in the past two years. His current research interests include SI, printed circuit board designs, circuit simulation, modeling of I/O devices and interconnects, multithreaded, and distributed computing.



**Ping Liu** was born in China in 1979. She received the B.S. and M.S. degrees in communications engineering from Beijing Jiao Tong University, Beijing, China, in 2000 and 2003, respectively, and the Ph.D. degree in electromagnetic fields and microwave engineering from Shanghai Jiao Tong University, Shanghai, China, in 2006.

She is currently with the Silicon Package Board Division, Cadence Design Systems Inc., Shanghai, working on the model extraction and circuit simulation tools research and development in high-speed circuits and systems. Her current research interests include field solver modeling of high-speed interconnects, large-scale circuit system simulation, and power and signal integrity analysis in high-speed circuits.